Am J Transl Res 2025;17(8):6236-6249
www.ajtr.org /ISSN:1943-8141/AJTR0165975

Original Article

Holdaway analysis exhibits the highest correlation with facial profile attractiveness among nine cephalometric analyses

Hongyu Ren, Xin Chen, Yongqing Zhang

Department of Orthodontics, Xiangyang Stomatological Hospital, Affiliated Stomatological Hospital of Hubei University of Arts and Science, Xiangyang, Hubei, China

Received May 12, 2025; Accepted July 25, 2025; Epub August 15, 2025; Published August 30, 2025

Abstract: Objective: To investigate the correlation between nine commonly used cephalometric analyses and facial profile attractiveness and to explore an optimized combination of cephalometric measures. Methods: Sixteen non-professional evaluators assessed the profile attractiveness of 210 untreated Chinese adults using a visual analog scale. Eighty-seven cephalometric measures were obtained from nine analyses (Burstone, Downs, Holdaway, Jarabak, McNamara, Ricketts, Steiner, Tweed, and Wylie). Quadratic regression analysis was employed to identify measures significantly correlated with facial profile attractiveness and to calculate their maximum attractiveness values (MAVs). Stepwise regression was applied to assess the explanatory power of each analysis for profile attractiveness and to construct optimized predictive models. Results: The explanatory power of the nine analyses for attractiveness variation was ranked as follows: Holdaway (41.5%) > Ricketts (37.6%) > Steiner (36.8%) > Burstone (35.7%) > Tweed (35.6%) > Downs (33.9%) > McNamara (24.3%) > Wylie (13.2%) > Jarabak (6.1%). Among individual measures, the H-angle, ANB (°), A-Npog (mm), and NA-APo (°) accounted for more than 26% of attractiveness variation. A five-indicator model comprising H-angle (28.8%; MAV = 17.2°), L1-APog (14.6%; MAV = 0.5 mm), Wits appraisal (4.5%; MAV = 0.1 mm), ANS-Me/N-Me (4.2%; MAV = 54%), and ANS-Ptm (3.3%; MAV = 46.7 mm) explained 55.4% of the variation. Conclusion: Among the nine cephalometric analyses, the Holdaway method exhibited the strongest explanatory power for variation in profile attractiveness. The newly constructed five-indicator model may provide more precise aesthetic references for orthodontic and orthognathic treatments.

Keywords: Cephalometric measurements, facial aesthetics, H-angle, Holdaway analysis, quadratic regression

Introduction

The focus of orthodontic treatment has shifted from merely improving occlusion to enhancing facial attractiveness [1-4]. However, quantitative assessment of facial aesthetic features remains a major challenge in clinical orthodontics and orthognathic treatment. Cephalometric analysis, a cornerstone of orthodontic diagnosis and treatment planning, has long provided essential quantitative data for clinicians to assess dentofacial development and formulate personalized treatment plans [5-8].

Nine widely used cephalometric analyses, Burstone, Downs, Holdaway, Jarabak, McNamara, Ricketts, Steiner, Tweed, and Wylie, each incorporate distinct indicators [9-12]. For example, the Ricketts analysis emphasizes overall craniofacial balance, whereas the Holdaway analysis focuses on lower facial third proportion and soft tissue balance [13]. Previous research has primarily explored the relationships between individual cephalometric analyses and facial attractiveness; however, it fails to provide comprehensive systematic comparisons among multiple methods [14]. Consequently, the strength of the correlation between these commonly used cephalometric analyses and facial attractiveness remains unclear.

Previous research examining the relationship between cephalometric measurements and facial aesthetics has predominantly relied on linear models [15-17]. However, emerging evi-

https://doi.org/10.62347/JSWV8973

Figure 1. Facial profile attractiveness assessment. A: A photograph used for assessment (written informed consent obtained from the patient for image publication); B: A visual analog scale used for scoring.

dence suggests that these traditional models fail to accurately capture the complex relationship between cephalometric measures and facial attractiveness [18]. Godinho et al. [18] identified a strong quadratic relationship between cephalometric measures and facial attractiveness, significantly outperforming linear correlations. On the basis of the parabolic characteristics of quadratic functions, they introduced the concept of the maximum attractiveness value (MAV) for cephalometric measures. For orthodontists and orthognathic surgeons concerned with facial aesthetics, the MAV offers substantial clinical value by serving as a reference target for optimization, thereby facilitating adjustments to achieve optimal aesthetic outcomes.

Building on this framework, the present study compared the correlations between nine commonly used cephalometric analyses and facial profile attractiveness using quadratic and stepwise regression. Additionally, it sought to establish an optimized combination of cephalometric measures to improve predictive accuracy. These findings are expected to guide clinicians in selecting analytical methods tailored to patients' aesthetic needs, thereby enhancing precision and scientific rigor in dentofacial treatment planning.

Materials and methods

Sample selection

This cross-sectional study was approved by the Ethics Committee of Xiangyang Stomatological Hospital (K24-006). The sample consisted of 105 Chinese males (average age: 25.3±4.8 years) and 105 Chinese females (average age: 26.4±5.1 years). Each sex group included 35 patients for each malocclusion category: Class I (0° ≤ ANB ≤ 4°), Class II (ANB > 4°), and Class III (ANB < 0°) [18].

Inclusion criteria: (1) age between 18 and 40 years; (2) no history of orthodontic or orthognathic treatment; (3) intact dentition; and (4) absence of apparent craniofacial deformities.

Facial photography and cephalometric radiography

Facial images were captured using a Nikon D80 digital single-lens reflex camera (Nikon Corporation, Tokyo, Japan). Patients were placed in a natural head position with mandibular maximum intercuspation and relaxed lips. Makeup, jewelry, glasses, and other interferences were removed (**Figure 1A**). To ensure consistency, the photographer positioned the camera at the Frankfort horizontal plane height with a 2.0 m shooting distance. Lateral cephalometric radiographs were obtained using an OC200D unit (Instrumentarium Dental, Turku, Finland), with the head's sagittal plane perpendicular to the X-ray central line and the Frankfort horizontal plane parallel to the ground. Head stabilization was achieved using a cephalostat, maintaining a tube-film distance of at least 150 cm to minimize magnification errors.

Assessment of facial profile attractiveness

A panel of 16 Chinese lay evaluators (8 males and 8 females; mean age: 32.4±8.6 years) assessed the facial profile attractiveness of

210 patients using standardized photographs and a visual analog scale (VAS). The evaluators were recruited from diverse age groups and occupational backgrounds, ensuring sample representativeness. The VAS consisted of a 100-mm horizontal line anchored at the left end with "0" (very unattractive) and at the right end with "10" (very attractive). The evaluators marked the line according to their subjective judgment (**Figure 1B**). The attractiveness score for each patient was determined by measuring the distance (in millimeters) from the 0 point to the evaluator's mark. The final scores were calculated as the mean value across all the evaluators. The intraclass correlation coefficient (ICC) for inter-rater reliability was 0.83, indicating good reliability.

Cephalometric measurements

Nine classic cephalometric analyses (Burstone, Downs, Holdaway, Jarabak, McNamara, Ricketts, Steiner, Tweed, and Wylie) were employed, encompassing 87 measures addressing key anatomical landmarks and indicators (**Table 1**). Three orthodontists independently measured digital lateral cephalograms using the Uceph analysis system (Dental Technology Co., Ltd., Chengdu, China) with resolution values of 0.1 mm and 0.1°. The final measured value was calculated as the mean value of independent measurements obtained by the three orthodontists. The ICCs for all cephalometric measures among the three orthodontists exceeded 0.90, meeting the criterion for high-reliability standards.

Statistical analysis

Statistical analyses were conducted using SPSS 22.0 software (IBM Corp., Armonk, NY, USA). Quadratic regression analysis was employed to identify measures significantly correlated with facial profile attractiveness and to calculate their MAVs ($P < 0.01$). The MAVs for these measures were computed using the vertex formula $-b/(2a)$ derived from the quadratic function $f(x) = ax^2 + bx + c$ [18]. For subsequent stepwise regression, significantly correlated measures were transformed into variables that demonstrated significant linear associations with profile attractiveness through an optimized MAV-based methodology [16]. Each original measurement value ($V1$) was converted to $V2 = |V1 - \text{MAV}|$, generating new variables reflecting absolute deviations from the MAV. Pearson correlation analysis was then performed to confirm that the transformed variables retained significant associations with attractiveness ($P < 0.01$) and that the correlation strength was not markedly reduced (r value decrease < 0.1). Stepwise regression was conducted to assess the explanatory power of the nine cephalometric analyses and to construct new predictive models. The regression parameters were set with an inclusion threshold of $P < 0.01$ and an exclusion threshold of $P > 0.10$.

Sample size estimation was based on a two-sided significance level of $\alpha = 0.01$ (two-sided test) and a test power of $1 - \beta = 0.95$. On the basis of Cohen's medium effect size standard ($r = 0.3$), the theoretical minimum sample size was calculated to be 189 participants using PASS 15.0.5 software (NCSS LLC, Kaysville, UT, USA). To ensure a balanced sex distribution and coverage of Class I-III malocclusions, a total of 210 patients were enrolled in the study.

Results

Descriptive statistics of the cephalometric measures

Table 2 presents the descriptive statistics, quadratic correlations with profile attractiveness, and MAVs for all cephalometric measures across the nine analyses. Among the 87 cephalometric measures, 39 demonstrated statistically significant quadratic relationships with profile attractiveness. **Figure 2** presents quadratic scatter plots illustrating the correlations between profile attractiveness and four key measures: H-angle, ANB (°), A-Npog (mm), and NA-APo (°).

MAV-based quadratic-to-linear correlation transformation

As shown in **Figure 2**, scatter plots of the quadratic correlations revealed that increased deviation from the MAV was associated with reduced facial attractiveness. To enable subsequent stepwise regression, significantly correlated measures were transformed into variables that demonstrated significant linear associations with attractiveness using an optimized MAV-based methodology [16]. **Table 3**

Table 1. Definition of the cephalometric measures

Analysis	Measure	Definition
Burstone	G-Pg' (mm)	Horizontal distance from Glabella (G) to soft tissue Pogonion (Pg')
Burstone	Sn-Gn'-C (°)	Angle formed by Subnasale (Sn), soft tissue Gnathion (Gn'), and Cervical point (C)
Burstone	G-Sn-Pg' (°)	Angle formed by Glabella (G), Subnasale (Sn), and soft tissue Pogonion (Pg')
Burstone	Ls-SnPg' (mm)	Perpendicular distance from Labrale superius (Ls) to the Sn-Pg' plane
Burstone	G-Sn/Sn-Me' (%)	Ratio of upper facial height (G-Sn) to lower facial height (Sn-Me')
Burstone	Sn-Gn'/C-Gn' (%)	Ratio of chin height (Sn-Gn') to cervical depth (C-Gn')
Burstone	G-Sn (mm)	Horizontal distance from Glabella (G) to Subnasale (Sn)
Burstone	Cm-Sn-Ls (°)	Nasolabial angle formed by Columella (Cm), Subnasale (Sn), and Labrale superius (Ls)
Burstone	Si-LiPg' (mm)	Distance from Mentolabial sulcus (Si) to Li-Pg' plane (a line related to the lower lip and soft tissue Pogion)
Burstone	Sn-Stms/Stmi-Me' (%)	Ratio of upper lip length (Sn-Stms) to lower lip-chin height (Stmi-Me')
Burstone	Stms-U1 (mm)	Distance from upper lip stomion (Stomion superius) to maxillary incisor edge
Burstone	Li-SnPg' (mm)	Perpendicular distance from Labrale inferius (Li) to the Sn-Pg' plane
Burstone	Stms-Stmi (mm)	Vertical height of lip interlabial gap (Stomion superius to Stomion inferius)
Downs	NA-APo (°)	Angle between NA line (Nasion-A point (Subspinale)) and APo line (A point-Pogonion)
Downs	AB-NPo (°)	Angle between AB line (A point-B point (Supramentale)) and NPo line (Nasion-Pogonion)
Downs	FH-NPo (°)	Frankfort Horizontal plane to Nasion-Pogonion plane angle
Downs	U1-APo (mm)	Distance from maxillary incisor edge to APo line
Downs	L1-OP (°)	Mandibular incisor long axis to Occlusal Plane angle
Downs	L1-MP (°)	Mandibular incisor long axis to Mandibular Plane angle
Downs	U1-L1 (°)	Interincisal angle between maxillary and mandibular incisors
Downs	SGn-FH (°)	Angle between Sella-Gnathion line and Frankfort Horizontal plane
Downs	FH-MP (°)	Frankfort Horizontal to Mandibular Plane angle
Downs	OP-FH (°)	Occlusal Plane to Frankfort Horizontal plane angle
Holdaway	H-angle (°)	Angle between soft tissue Nasion-Pogonion line and H-line (upper lip tangent)
Holdaway	A-Npog (mm)	Distance from skeletal A point to Nasion-Pogonion line
Holdaway	FH-N'Pog' (°)	Frankfort Horizontal to soft tissue Nasion'-Pogonion' angle
Holdaway	Sn-H (mm)	Distance from Subnasale to H-line
Holdaway	Si-H (mm)	Distance from Mentolabial sulcus (Si) to H-line
Holdaway	Li-H (mm)	Distance from Labrale inferius to H-line
Holdaway	Prn-Sn (mm)	Nasal tip length from Pronasale to Subnasale
Holdaway	Pm-Pm' (mm)	Distance from hard tissue Pogonion to soft tissue Pogonion
Holdaway	Ss-Ls (mm)	Upper lip length from Subnasale stomion to Labrale superius
Holdaway	FA (U1)-Ls (mm)	Distance from maxillary incisor facial axis (FA) to Labrale superius
Jarabak	S-N/Go'-Me (%)	Ratio of distance from Sella (S) to Nasion (N) to distance from a modified Gonion (Go') to Menton (Me)
Jarabak	Go'-Me (mm)	Distance from a modified Gonion (Go') to Menton (Me)
Jarabak	S+Ar+Go (°)	Sum of angles at Sella, Articulare, and Gonion
Jarabak	S-Go'/N-Me (%)	Ratio of posterior facial height (S-Go') to anterior facial height (N-Me)
Jarabak	Ar-Go'-Me (°)	Gonial angle at Gonion between Articulare, a modified Gonion, and Menton
Jarabak	N-Me (mm)	Anterior total facial height from Nasion to Menton
Jarabak	N-S-Ar (°)	Cranial base angle at Sella between Nasion, Sella, and Articulare
Jarabak	N-Go'-Me (°)	Angle formed by Nasion, a modified Gonion, and Menton
Jarabak	Ar-Go' (mm)	Distance from Articulare to a modified Gonion (ramus length)

Jarabak	S-Ar/Ar-Go' (%)	Ratio of posterior cranial base (S-Ar) to ramus height (Ar-Go')
Jarabak	S-Go' (mm)	Posterior facial height from Sella to a modified Gonion
Jarabak	Ar-S (mm)	Distance from Articulare to Sella
Jarabak	Ar-Go'-N (°)	Angle at Gonion between Articulare, a modified Gonion, and Nasion
Jarabak	S-N (mm)	Anterior cranial base length from Sella to Nasion
Jarabak	S-Ar-Go' (°)	Angle at Articulare between Sella, Articulare, and a modified Gonion
Ricketts	A-Npog (mm)	Distance from skeletal A point to Nasion-Pogonion line
Ricketts	L1-APog (mm)	Distance from mandibular incisor edge to A point-Pogonion line
Ricketts	FH-NPo (°)	Frankfort Horizontal plane to Nasion-Pogonion plane angle
Ricketts	U1-APo (mm)	Distance from maxillary incisor edge to APo line
Ricketts	NBa-PtGn (°)	Angle between the cranial base (Nasion-Basion) and mandibular plane (Pterion-Gnathion)
Ricketts	LL-EP (mm)	Lower lip position relative to Esthetic Plane (line from nasal tip to soft tissue Pogonion)
Ricketts	L1-APog (°)	Mandibular incisor inclination to A point-Pogonion line
Ricketts	FH-MP (°)	Frankfort Horizontal to Mandibular Plane angle
Ricketts	MP-NPog (°)	Mandibular Plane to Nasion-Pogonion angle
Wylie	N-ANS/N-Me (%)	Ratio of upper anterior facial height (Nasion-Anterior Nasal Spine) to total anterior facial height (Nasion-Menton)
Wylie	ANS-Me/N-Me (%)	Ratio of lower anterior facial height (Anterior Nasal Spine-Menton) to total anterior facial height
Wylie	ANS-Ptm (mm)	Maxillary length from Anterior Nasal Spine to Pterygomaxillary fissure
Wylie	Ptm-U6 (mm)	Distance from Pterygomaxillary fissure to the maxillary first molar
Wylie	Co-Po (mm)	Mandibular body length from Condylion to Pogonion
Wylie	ANS-Me (mm)	Lower anterior facial height from Anterior Nasal Spine to Menton
Wylie	Co-S (mm)	Distance from Condylion to Sella
Wylie	S-Ptm (mm)	Posterior maxillary length from Sella to Pterygomaxillary fissure
Wylie	N-Me (mm)	Total anterior facial height from Nasion to Menton
Wylie	N-ANS (mm)	Upper anterior facial height from Nasion to Anterior Nasal Spine
McNamara	L1-APog (mm)	Distance from mandibular incisor edge to A point-Pogonion line
McNamara	Pog-Np (mm)	Horizontal distance from Pogonion (Pog) to Nasion perpendicular line (Np)
McNamara	ANS-Me (mm)	Lower anterior facial height from Anterior Nasal Spine to Menton
McNamara	U1-A (mm)	Horizontal distance from maxillary incisor edge to A point
McNamara	A-Np (mm)	Horizontal distance from A point to Nasion perpendicular line (Np)
McNamara	Co-Gn (mm)	Mandibular length from Condylion to Gnathion
McNamara	Co-A (mm)	Maxillary length from Condylion to A point
Steiner	ANB (°)	Angle between NA and NB lines (maxillomandibular discrepancy)
Steiner	SND (°)	Angle between Sella-Nasion line and Nasion-Dens line
Steiner	SNB (°)	Angle between Sella-Nasion line and Nasion-B point (mandibular position)
Steiner	L1-NB (mm)	Distance from mandibular incisor edge to NB line
Steiner	L1-NB (°)	Mandibular incisor inclination to NB line
Steiner	U1-L1 (°)	Interincisal angle between maxillary and mandibular incisors
Steiner	SNA (°)	Angle between Sella-Nasion line and Nasion-A point (maxillary position)
Steiner	SL (mm)	Distance from Pogonion to Perpendicular of Sella-Nasion line passing through Nasion
Steiner	OP-SN (°)	Occlusal Plane to Sella-Nasion plane angle
Steiner	Po-NB (mm)	Distance from Pogonion to NB line
Steiner	GoGn-SN (°)	Mandibular plane (Gonion-Gnathion) to Sella-Nasion plane angle
Steiner	U1-NA (mm)	Distance from maxillary incisor edge to NA line
Steiner	U1-NA (°)	Maxillary incisor inclination to NA line

Steiner	SE (mm)	Distance from Postcondylare to Perpendicular of Sella-Nasion line passing through Sella
Tweed	ANB (°)	Angle between NA and NB lines (maxillomandibular discrepancy)
Tweed	AO-BO (Wits mm)	Occlusal plane projection difference between A point and B point (Wits appraisal)
Tweed	Z-Angle (°)	Angle between Frankfort Horizontal and soft tissue profile line (Z-line)
Tweed	SNB (°)	Angle between Sella-Nasion line and Nasion-B point (mandibular position)
Tweed	FMIA (°)	Frankfort Mandibular Incisor Angle (L1 to FH plane)
Tweed	L1-MP (°)	Mandibular incisor long axis to Mandibular Plane angle
Tweed	SNA (°)	Angle between Sella-Nasion line and Nasion-A point (maxillary position)
Tweed	FH-MP (°)	Frankfort Horizontal to Mandibular Plane angle
Tweed	PFH/AFH (%)	Ratio of posterior facial height (Articulare-a modified Gonion) to anterior facial height (Anterior Nasal Spine-Menton)
Tweed	AFH (mm)	Anterior facial height (Anterior Nasal Spine-Menton)
Tweed	Ar-Go' (mm)	Distance from Articulare to a modified Gonion (ramus length)
Tweed	OP-FH (°)	Occlusal Plane to Frankfort Horizontal plane angle

Table 2. Descriptive statistics, quadratic correlations with profile attractiveness, and maximum attractiveness values (MAVs) of the cephalometric measures

Analysis	Measure	Range	Mean ± SD	*r*	*P*	MAV
Burstone	G-Pg' (mm)	-28.7-24.8	-4.2±8.4	0.371*	< 0.001	-6.6
Burstone	Sn-Gn'-C (°)	72.6-135.6	98.8±10.3	0.359*	< 0.001	105.7
Burstone	G-Sn-Pg' (°)	0-30.7	10.2±6.7	0.348*	< 0.001	12.7
Burstone	Ls-SnPg' (mm)	1-13.6	6.7±2.3	0.328*	< 0.001	6
Burstone	G-Sn/Sn-Me' (%)	83.8-132.1	104.7±8.8	0.295*	0.002	115.9
Burstone	Sn-Gn'/C-Gn' (%)	100.1-213.9	141.5±19	0.2	0.014	-
Burstone	G-Sn (mm)	-8.3-12.2	2.5±3.6	0.187	0.017	-
Burstone	Cm-Sn-Ls (°)	69.6-128.6	97.9±11	0.283	0.017	-
Burstone	Si-LiPg' (mm)	0.3-8.5	4.4±1.5	0.226	0.023	-
Burstone	Sn-Stms/Stmi-Me' (%)	33.3-60	45.4±4.5	0.199	0.041	-
Burstone	Stms-U1 (mm)	-2.5-6.8	2.3±1.7	0.232	0.049	-
Burstone	Li-SnPg' (mm)	-1-18	6.1±2.7	0.366	0.086	-
Burstone	Stms-Stmi (mm)	1.1-3.3	1.8±0.3	0.034	0.638	-
Downs	NA-APo (°)	-20.5-22	3.8±8.8	0.471*	< 0.001	4
Downs	AB-NPo (°)	-15.2-12.4	-3.8±6	0.458*	< 0.001	-4.6
Downs	FH-NPo (°)	80-99.5	89.3±4	0.354*	< 0.001	88.7
Downs	U1-APo (mm)	-1.2-19.1	7.4±3.6	0.347*	< 0.001	7.1
Downs	L1-OP (°)	87.5-132.8	111.9±8.1	0.333*	< 0.001	108.4
Downs	L1-MP (°)	65.3-113.4	94±8.7	0.293*	< 0.001	95.5
Downs	U1-L1 (°)	95-162.6	126.6±12.3	0.271*	< 0.001	133.7
Downs	SGn-FH (°)	51.6-70.8	60.8±3.8	0.243*	0.001	62.2
Downs	FH-MP (°)	6.9-39.7	23.4±6.1	0.17	0.026	-
Downs	OP-FH (°)	0-17.3	6±3.8	0.035	0.675	-
Holdaway	H-angle (°)	2.2-31.5	17.3±5.8	0.5*	< 0.001	17.2
Holdaway	A-Npog (mm)	-8.9-11	1.9±4.3	0.494*	< 0.001	2
Holdaway	FH-N'Pog' (°)	81.7-103.7	93±4.2	0.356*	< 0.001	92.5
Holdaway	Sn-H (mm)	1.4-16.4	9.1±2.9	0.324*	< 0.001	8.1
Holdaway	Si-H (mm)	-4.7-8.4	3.3±2.2	0.385*	0.001	5.3
Holdaway	Li-H (mm)	-4-9.2	1.9±2.1	0.389*	0.004	-0.9

Holdaway	Prn-Sn (mm)	6.1-17.2	12.7±1.7	0.118	0.122	-
Holdaway	Pm-Pm' (mm)	6.4-17.8	11.5±1.9	0.112	0.127	-
Holdaway	Ss-Ls (mm)	-0.5-6.8	3.6±1.2	0.205	0.441	-
Holdaway	FA (U1)-Ls (mm)	5.8-23.1	12.2±2.4	0.091	0.58	-
Jarabak	S-N/Go'-Me (%)	75.5-110.5	90.6±6.4	0.251*	< 0.001	92.7
Jarabak	Go'-Me (mm)	55.8-87.6	70.1±5.2	0.25*	0.002	68.7
Jarabak	S+Ar+Go (°)	373.1-411.8	392.8±6.8	0.154	0.026	-
Jarabak	S-Go'/N-Me (%)	52-86.2	68±5.5	0.137	0.057	-
Jarabak	Ar-Go'-Me (°)	100.1-139.1	118.3±7.1	0.188	0.201	-
Jarabak	N-Me (mm)	90.8-139.6	117.3±8	0.101	0.244	-
Jarabak	N-S-Ar (°)	111.9-138.8	124.2±5.1	0.228	0.261	-
Jarabak	N-Go'-Me (°)	59.3-88.6	74.3±5.6	0.123	0.3	-
Jarabak	Ar-Go' (mm)	34-67.6	48.3±5.6	0.062	0.383	-
Jarabak	S-Ar/Ar-Go' (%)	45.6-98.9	71.6±8.3	0.056	0.433	-
Jarabak	S-Go' (mm)	58.6-104.6	79.7±7.6	0.051	0.46	-
Jarabak	Ar-S (mm)	25.1-44	34.3±3.6	0.051	0.471	-
Jarabak	Ar-Go'-N (°)	34.6-57.1	44±3.8	0.17	0.534	-
Jarabak	S-N (mm)	49.2-73.2	63.3±3.7	0.147	0.606	-
Jarabak	S-Ar-Go' (°)	132.2-166.4	150.3±6.7	0.024	0.769	-
Ricketts	A-Npog (mm)	-8.9-11	1.9±4.3	0.494*	< 0.001	2
Ricketts	L1-APog (mm)	-4.1-12.6	3.9±3	0.395*	< 0.001	0.5
Ricketts	FH-NPo (°)	80-99.5	89.3±4	0.354*	< 0.001	88.7
Ricketts	U1-APo (mm)	-1.2-19.1	7.4±3.6	0.347*	< 0.001	7.1
Ricketts	NBa-PtGn (°)	74.3-98.3	86±4.7	0.275*	< 0.001	83.4
Ricketts	LL-EP (mm)	-7-14.4	1.7±3.2	0.304*	0.003	-1.2
Ricketts	L1-APog (°)	8.2-37.9	24.7±5.4	0.252*	0.004	20.5
Ricketts	FH-MP (°)	6.9-39.7	23.4±6.1	0.17	0.026	-
Ricketts	MP-NPog (°)	53.3-82.4	67.4±5.1	0.225	0.07	-
Wylie	N-ANS/N-Me (%)	40.3-50	45±1.9	0.277*	< 0.001	46
Wylie	ANS-Me/N-Me (%)	50-59.7	55±1.9	0.277*	< 0.001	54
Wylie	ANS-Ptm (mm)	36-54.8	47.7±3.3	0.243*	0.001	46.7
Wylie	Ptm-U6 (mm)	11.3-28.3	21±3.2	0.257	0.025	-
Wylie	Co-Po (mm)	76.2-120.4	97.7±7.6	0.276	0.033	-
Wylie	ANS-Me (mm)	48.5-81.3	64.3±5.7	0.158	0.068	-
Wylie	Co-S (mm)	4.9-15.6	10.3±2.3	0.162	0.128	-
Wylie	S-Ptm (mm)	13-24.4	19.3±2.3	0.145	0.221	-
Wylie	N-Me (mm)	90.4-138.7	116.8±7.9	0.089	0.304	-
Wylie	N-ANS (mm)	39.1-61.9	52.5±3.3	0.055	0.585	-
McNamara	L1-APog (mm)	-4.1-12.6	3.9±3	0.395*	< 0.001	0.5
McNamara	Pog-Np (mm)	-19.4-19.4	-1.5±7.8	0.361*	< 0.001	-2.6
McNamara	ANS-Me (mm)	49.6-82.5	66±5.9	0.191	0.017	-
McNamara	U1-A (mm)	-2-14.6	6.3±3	0.238	0.023	-
McNamara	A-Np (mm)	-7.9-9.9	1.1±3.2	0.162	0.026	-
McNamara	Co-Gn (mm)	85.2-134.5	110.4±7.8	0.224	0.036	-
McNamara	Co-A (mm)	63.4-92.3	79.4±5	0.13	0.078	-
Steiner	ANB (°)	-7.9-9.9	2.2±3.9	0.504*	< 0.001	2.3
Steiner	SND (°)	66.8-92.8	76.9±4.4	0.37*	< 0.001	75.1
Steiner	SNB (°)	69.8-94.6	79.4±4.4	0.368*	< 0.001	76.7
Steiner	L1-NB (mm)	-2.4-16.7	5.6±3.2	0.331*	< 0.001	5.2

Steiner	L1-NB (°)	3.6-47.8	26.2±8.1	0.323*	< 0.001	25.4
Steiner	U1-L1 (°)	95-162.6	126.6±12.3	0.271*	< 0.001	133.7
Steiner	SNA (°)	71.2-92.4	81.6±3.3	0.255*	< 0.001	80.2
Steiner	SL (mm)	23.1-80.7	43.6±9.4	0.312*	0.003	38.6
Steiner	OP-SN (°)	0.7-27.2	15±5	0.235*	0.006	17.2
Steiner	Po-NB (mm)	-3.2-5.9	0.8±1.8	0.244	0.021	-
Steiner	GoGn-SN (°)	13.3-49.7	32±6.2	0.143	0.039	-
Steiner	U1-NA (mm)	-4.6-14.7	5.8±3	0.226	0.102	-
Steiner	U1-NA (°)	0.5-46.5	25±8.1	0.209	0.137	-
Steiner	SE (mm)	13.1-25.2	18.8±2.6	0.199	0.568	-
Tweed	ANB (°)	-7.9-9.9	2.2±3.9	0.504*	< 0.001	2.3
Tweed	AO-BO (Wits mm)	-12.8-8.7	-0.6±4.8	0.438*	< 0.001	0.1
Tweed	Z-Angle (°)	51.4-95.6	74.1±7.8	0.373*	< 0.001	74.8
Tweed	SNB (°)	69.8-94.6	79.4±4.4	0.368*	< 0.001	76.7
Tweed	FMIA (L1-FH) (°)	33.9-88.7	62.6±10.1	0.348*	< 0.001	62.3
Tweed	L1-MP (°)	65.3-113.4	94±8.7	0.293*	< 0.001	95.5
Tweed	SNA (°)	71.2-92.4	81.6±3.3	0.255*	< 0.001	80.2
Tweed	FH-MP (°)	6.9-39.7	23.4±6.1	0.17	0.026	-
Tweed	PFH/AFH (%)	53.9-110	75.3±8.6	0.147	0.044	-
Tweed	AFH (mm)	48.5-81.4	64.3±5.7	0.164	0.053	-
Tweed	Ar-Go' (mm)	34-67.6	48.3±5.6	0.062	0.383	-
Tweed	OP-FH (°)	0-17.3	6±3.8	0.035	0.675	-

*$P < 0.01$.

summarizes the results of this transformation. All transformed variables exhibited significant linear correlations with facial attractiveness. Notably, for the seven most influential measures ($r1 \geq 0.395$), the transformed linear correlation coefficients ($r2$) exceeded the original quadratic correlation coefficients ($r1$). This indicates an advantage gradient where the transformation efficacy increased with increasing initial quadratic correlations. Overall, 16 measures exhibited increased correlation coefficients after transformation. Among the remaining 23 measures showing decreased correlations, 17 exhibited reductions < 0.02, 4 showed decreases of 0.031-0.040, and only 2 exceeded 0.04 (0.044 and 0.068). These results confirm that the MAV-based quadratic-to-linear transformation preserved statistical significance in all measures (39/39, 100%) while maintaining or enhancing correlation strength in most cases, validating the method's reliability and practicality.

Explanatory power of each analysis for variation in profile attractiveness

After confirming that the MAV-based transformation preserved both statistical significance and correlation strength of the original measures, stepwise regression was applied to assess the explanatory power of each analysis for profile attractiveness and to construct optimized predictive models. The explanatory power of each analysis for variation in profile attractiveness was calculated via the *r*-squared (r^2) values obtained from stepwise regression. The variation in profile attractiveness explained by the nine cephalometric analyses was ranked as follows: Holdaway (41.5%) > Ricketts (37.6%) > Steiner (36.8%) > Burstone (35.7%) > Tweed (35.6%) > Downs (33.9%) > McNamara (24.3%) > Wylie (13.2%) > Jarabak (6.1%) (**Table 4**).

Construction of four new predictive models for profile attractiveness

Among the 39 transformed cephalometric variables, H-angle, ANB (°), A-Npog (mm), and NA-APo (°) exhibited the strongest linear correlation with facial attractiveness (**Table 3**). Pearson correlation analysis confirmed significant intercorrelations ($P < 0.01$) among their original measurements (**Table 5**). Consequently, we developed four new predictive models using stepwise regression, with H-angle, ANB

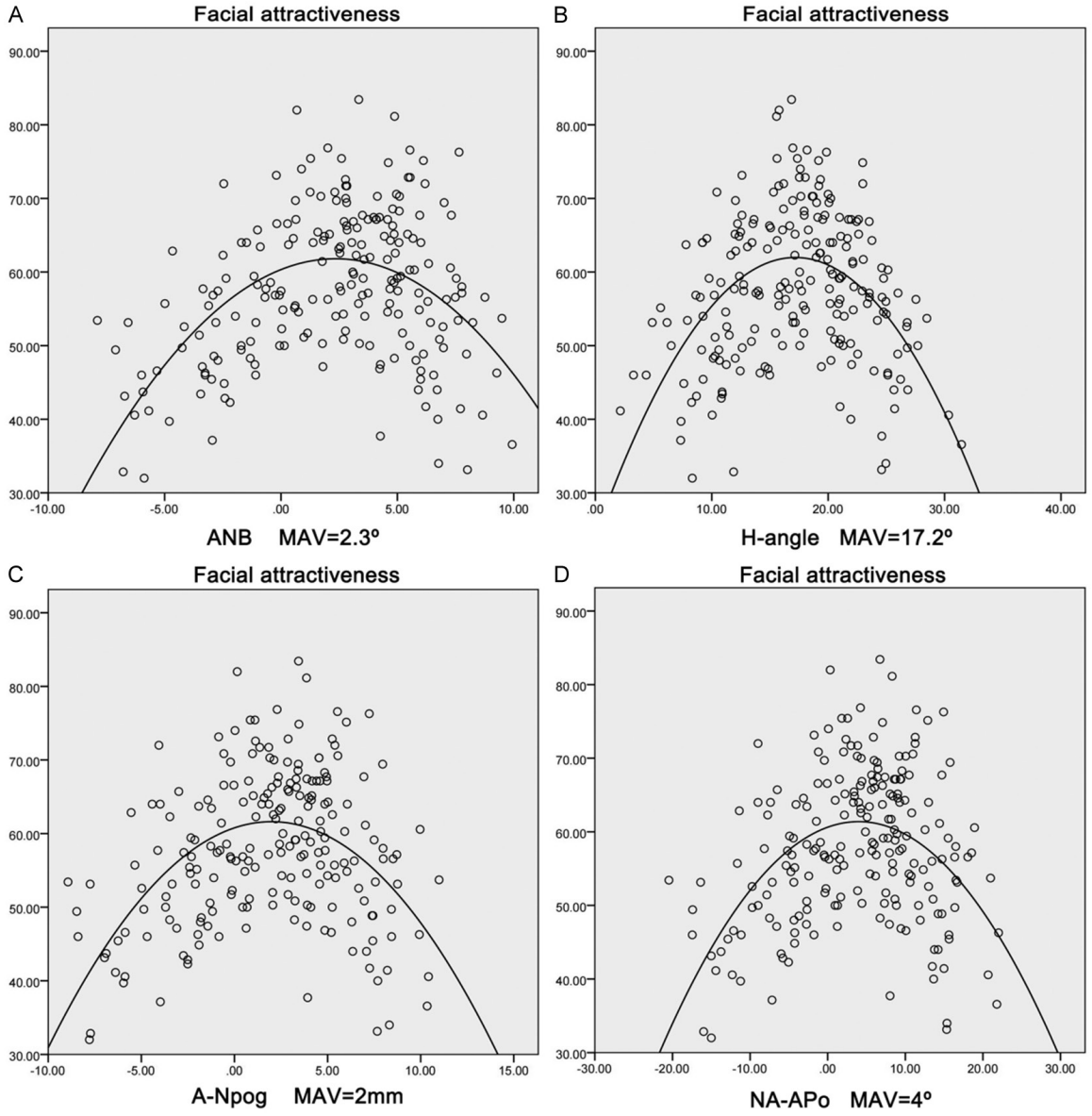

Figure 2. Scatter plots of the quadratic correlations between profile attractiveness and ANB (A), H-angle (B), A-Npog (C), and NA-APo (D). MAV: maximum attractiveness value.

(°), A-Npog (mm), and NA-APo (°) as the primary predictors (**Table 6**). For example, the combination of H-angle (r^2 partial = 28.8%, MAV = 17.2°), L1-APog (r^2 partial = 14.6%, MAV = 0.5 mm), Wits appraisal (r^2 partial = 4.5%, MAV = 0.1 mm), ANS-Me/N-Me (r^2 partial = 4.2%, MAV = 54%), and ANS-Ptm (r^2 partial = 3.3%, MAV = 46.7 mm) explained 55.4% of the variation in attractiveness. Notably, H-angle, ANB (°), A-Npog (mm), and NA-APo (°) each individually explained over 26% of the variation in attractiveness ($r^2 > 0.26$).

Discussion

The strength of the correlation between commonly used cephalometric analyses and facial attractiveness remains unclear. This study systematically compared, for the first time, correlations between nine commonly used cephalometric analyses and profile attractiveness and optimized combination of cephalometric measures.

Among the 87 cephalometric measures evaluated, 39 showed a significant quadratic correla-

Table 3. Thirty-nine cephalometric measures demonstrating significant quadratic correlations with profile attractiveness and their maximum attractiveness value (MAV)-based linear transformations. The ranking of the cephalometric measures is based on the magnitude of the difference between |*r2*| and *r1*

Order	Measure	Quadratic correlation			Linear correlation			Difference
		r1	*P*	MAV	*r2*	|*r2*|	*P*	|*r2*|-*r1*
1	L1-MP (°)[D,T]	0.293	< 0.001	95.5	-0.34	0.34	< 0.001	0.047
2	G-Sn-Pg' (°)[B]	0.348	< 0.001	12.7	-0.388	0.388	< 0.001	0.04
3	NA-APo (°)[D]	0.471	< 0.001	4	-0.51	0.51	< 0.001	0.039
4	H-angle (°)[H]	0.5	< 0.001	17.2	-0.537	0.537	< 0.001	0.037
5	FMIA (L1-FH)[T]	0.348	< 0.001	62.3	-0.377	0.377	< 0.001	0.029
6	A-Npog (mm)[H,R]	0.494	< 0.001	2	-0.52	0.52	< 0.001	0.026
7	ANB (°)[S,T]	0.504	< 0.001	2.3	-0.528	0.528	< 0.001	0.024
8	AO-BO (Wits mm)[T]	0.438	< 0.001	0.1	-0.461	0.461	< 0.001	0.023
9	AB-NPo (°)[D]	0.458	< 0.001	-4.6	-0.476	0.476	< 0.001	0.018
10	Z-Angle (°)[T]	0.373	< 0.001	74.8	-0.39	0.39	< 0.001	0.017
11	U1-APo (mm)[D,R]	0.347	< 0.001	7.1	-0.364	0.364	< 0.001	0.017
12	L1-APog (mm)[M,R]	0.395	< 0.001	0.5	-0.404	0.404	< 0.001	0.009
13	L1-NB (mm)[S]	0.331	< 0.001	5.2	-0.34	0.34	< 0.001	0.009
14	L1-NB (°)[S]	0.323	< 0.001	25.4	-0.332	0.332	< 0.001	0.009
15	ANS-Ptm (mm)[W]	0.243	0.001	46.7	-0.247	0.247	< 0.001	0.004
16	SGn-FH (°)[D]	0.243	0.001	62.2	-0.245	0.245	< 0.001	0.002
1	L1-OP (°)[D]	0.333	< 0.001	108.4	-0.265	0.265	< 0.001	-0.068
2	NBa-PtGn (°)[R]	0.275	< 0.001	83.4	-0.231	0.231	0.001	-0.044
3	Go'-Me (mm)[J]	0.25	0.002	68.7	-0.21	0.21	0.002	-0.04
4	SNA (°)[S,T]	0.255	< 0.001	80.2	-0.217	0.217	0.002	-0.038
5	Sn-Gn'-C (°)[B]	0.359	< 0.001	105.7	-0.325	0.325	< 0.001	-0.034
6	U1-L1 (°)[D,S]	0.271	< 0.001	133.7	-0.24	0.24	< 0.001	-0.031
7	SL (mm)[S]	0.312	0.003	38.6	-0.293	0.293	< 0.001	-0.019
8	G-Pg' (mm)[B]	0.371	< 0.001	-6.6	-0.354	0.354	< 0.001	-0.017
9	SND (°)[S]	0.37	< 0.001	75.1	-0.353	0.353	< 0.001	-0.017
10	SNB (°)[S,T]	0.368	< 0.001	76.7	-0.351	0.351	< 0.001	-0.017
11	Sn-H (mm)[H]	0.324	< 0.001	8.1	-0.307	0.307	< 0.001	-0.017
12	G-Sn/Sn-Me' (%)[B]	0.295	0.002	115.9	-0.278	0.278	< 0.001	-0.017
13	L1-APog (°)[R]	0.252	0.004	20.5	-0.236	0.236	0.001	-0.016
14	LL-EP (mm)[R]	0.304	0.003	-1.2	-0.289	0.289	< 0.001	-0.015
15	OP-SN (°)[S]	0.235	0.006	17.2	-0.22	0.22	0.001	-0.015
16	Pog-Np (mm)[M]	0.361	< 0.001	-2.6	-0.35	0.35	< 0.001	-0.011
17	FH-NPo (°)[D,R]	0.354	< 0.001	88.7	-0.346	0.346	< 0.001	-0.008
18	Li-H (Hmm)[H]	0.389	0.004	-0.9	-0.385	0.385	< 0.001	-0.004
19	FH-N'Pog' (°)[H]	0.356	< 0.001	92.5	-0.352	0.352	< 0.001	-0.004
20	S-N/Go'-Me (%)[J]	0.251	< 0.001	92.7	-0.247	0.247	< 0.001	-0.004
21	Si-H (mm)[H]	0.385	0.001	5.3	-0.382	0.382	< 0.001	-0.003
22	Ls-SnPg' (mm)[B]	0.328	< 0.001	6	-0.325	0.325	< 0.001	-0.003
23	ANS-Me/N-Me (%)[W]	0.277	< 0.001	54	-0.276	0.276	< 0.001	-0.001

[B]Burstone; [D]Downs; [H]Holdaway; [J]Jarabak; [M]McNamara; [R]Ricketts; [S]Steiner; [T]Tweed; [W]Wylie.

tion with profile attractiveness, with only nine related to the maxillary and mandibular incisors. These measures, ranked by *r* value, are L1-APog (mm, *r* = 0.395), L1-FH (°, *r* = 0.348),

Table 4. Explanatory power of each analysis for variation in profile attractiveness

Analysis	Measure	*r*	r^2 partial	r^2 cumulative	*P*
Holdaway	H-angle (°)	0.537	0.288	0.288	< 0.001
	Li-H (mm)	0.622	+0.099	0.387	< 0.001
	A-Npog (mm)	0.644	+0.028	0.415	0.002
Ricketts	A-Npog (mm)	0.52	0.27	0.27	< 0.001
	L1-APog (mm)	0.613	+0.106	0.376	< 0.001
Steiner	ANB (°)	0.528	0.279	0.279	< 0.001
	U1-L1 (°)	0.584	+0.062	0.341	< 0.001
	SNB (°)	0.607	+0.027	0.368	0.003
Burstone	G-Sn-Pg' (°)	0.388	0.15	0.15	< 0.001
	Ls-SnPg' (mm)	0.519	+0.119	0.269	< 0.001
	Sn-Gn'-C (°)	0.568	+0.053	0.322	< 0.001
	G-Sn/Sn-Me' (%)	0.598	+0.035	0.357	0.001
Tweed	ANB (°)	0.528	0.279	0.279	< 0.001
	Z-Angle (°)	0.554	+0.028	0.307	0.004
	AO-BO (Wits mm)	0.579	+0.028	0.335	0.004
	SNA (°)	0.597	+0.021	0.356	0.01
Downs	NA-APo (°)	0.51	0.26	0.26	< 0.001
	U1-L1 (°)	0.555	+0.048	0.308	< 0.001
	AB-NPo (°)	0.583	+0.031	0.339	0.002
McNamara	L1-APog (mm)	0.404	0.163	0.163	< 0.001
	Pog-Np (mm)	0.493	+0.08	0.243	< 0.001
Wylie	ANS-Me/N-Me (%)	0.276	0.076	0.076	< 0.001
	ANS-Ptm (mm)	0.363	+0.056	0.132	< 0.001
Jarabak	S-N/Go'-Me (%)	0.247	0.061	0.061	< 0.001

Table 5. Pearson correlation coefficients among H-angle, ANB (°), A-Npog (mm), and NA-APo (°)

Measure	NA-APo (°)	A-Npog (mm)	H-angle (°)	ANB (°)
NA-APo (°)	-	0.997*	0.836*	0.975*
A-Npog (mm)	-	-	0.837*	0.972*
H-angle (°)	-	-	-	0.809*

*$P < 0.01$.

U1-APo (mm, $r = 0.347$), L1-OP (°, $r = 0.333$), L1-NB (mm, $r = 0.331$), L1-NB (°, $r = 0.323$), L1-MP (°, $r = 0.293$), U1-L1 (°, $r = 0.271$), and L1-APog (°, $r = 0.252$). Notably, mandibular incisor indicators exerted a more significant effect than did maxillary incisor indicators, both in terms of the number of significant measures and the strength of correlation. This finding supports the orthodontic consensus that 3D positioning of mandibular incisors within the mandibular arch not only affects occlusion but also serves as a pivotal consideration for treatment planning [19].

The Tweed theory emphasizes the relationship between mandibular incisor inclination and the mandibular plane (MP), highlighting specific angular criteria for facial aesthetics [9]. However, this study revealed that the correlation coefficient for L1-MP (°, $r = 0.293$) was significantly lower than those of other measures, suggesting that its aesthetic predictive value may be overestimated. This discrepancy may stem from differences in sample composition. Research by Hernández-Sayago et al. [20] revealed significant differences in mandibular incisor inclination across various malocclusion classifications. It is speculated that Class I malocclusion patients may require more upright incisors to optimize aesthetics and maintain periodontal health, whereas Class II/III patients with sagittal jaw discrepancies may compensatory inclinations deviating from ideal. As this study included equal samples of Class I, II, and III patients, the mixed compensatory patterns likely attenuated the overall correlation between L1-MP (°) and profile attractiveness. Future research should use

Table 6. Construction of four new predictive models for profile attractiveness

Analysis	Measure	*r*	r^2 partial	r^2 cumulative	*P*
New 1	H-angle (°)	0.537	0.288	0.288	< 0.001
	L1-APog (mm)	0.659	+0.146	0.434	< 0.001
	AO-BO (Wits mm)	0.692	+0.045	0.479	< 0.001
	ANS-Me/N-Me (%)	0.722	+0.042	0.521	< 0.001
	ANS-Ptm (mm)	0.744	+0.033	0.554	< 0.001
New 2	ANB (°)	0.528	0.279	0.279	< 0.001
	L1-APog (mm)	0.618	+0.103	0.382	< 0.001
	ANS-Ptm (mm)	0.658	+0.051	0.433	< 0.001
	ANS-Me/N-Me (%)	0.685	+0.037	0.47	< 0.001
	Z-Angle (°)	0.711	+0.036	0.506	< 0.001
	Sn-Gn'-C (°)	0.732	+0.03	0.536	< 0.001
New 3	NA-APo (°)	0.51	0.26	0.26	< 0.001
	L1-APog (mm)	0.611	+0.114	0.374	< 0.001
	ANS-Ptm (mm)	0.652	+0.051	0.425	< 0.001
	ANS-Me/N-Me (%)	0.684	+0.043	0.468	< 0.001
	AO-BO (Wits mm)	0.711	+0.037	0.505	< 0.001
	Z-Angle (°)	0.73	+0.027	0.532	0.001
New 4	A-Npog (mm)	0.52	0.27	0.27	< 0.001
	L1-APog (mm)	0.613	+0.106	0.376	< 0.001
	ANS-Me/N-Me (%)	0.65	+0.047	0.423	< 0.001
	ANS-Ptm (mm)	0.682	+0.042	0.465	< 0.001
	AO-BO (Wits mm)	0.71	+0.039	0.504	< 0.001
	Z-Angle (°)	0.729	+0.027	0.531	0.001

models stratified by malocclusion type to assess the aesthetic significance of L1-MP (°).

This study revealed that the nine cephalometric analyses differed significantly in their explanatory power for variation in profile attractiveness. Among them, the Holdaway analysis demonstrated the strongest explanatory power, accounting for 41.5% of the variation in facial attractiveness. This may be due to its unique H-angle, which simultaneously reflects the coordination between the upper lip protrusion and chin morphology, aligning with the "chin-lip complex" aesthetic theory [14]. The explanatory power of the McNamara, Wylie, and Jarabak analyses was relatively low, at 24.3%, 13.2%, and 6.1%, respectively. These methods focused primarily on the absolute hard tissue dimensions and largely neglected soft tissue compensation, thereby limiting their ability to predict facial attractiveness. These results suggest that different cephalometric analyses exhibit clear hierarchical differences in their correlation with facial attractiveness, which has important implications for orthodontic and orthognathic treatments. For example, when patients have high demands for facial attractiveness, Holdaway analysis should be preferred for diagnostic assessment.

Although other unmeasured factors such as skin color, hairstyle, and facial expressions may influence facial attractiveness [21, 22], the H-angle, ANB (°), A-Npog (mm), and NA-APo (°) each explained over 26% of the attractiveness variation when analyzed individually, highlighting their core roles in facial aesthetics. The Pearson correlation coefficient results revealed strong correlations among these measures. Therefore, this study constructed four new predictive models for profile attractiveness, primarily on the basis of these four measures. Notably, the measures L1-APog (mm), ANS-Me/N-Me (%), and ANS-Ptm (mm) appeared in all four models, whereas Wits appraisal (mm) and Z-Angle appeared in three of them, demonstrating their stability in predicting profile attractiveness.

Further analysis revealed that the new predictive model, which integrated H-angle, L1-APog

(mm), Wits appraisal (mm), ANS-Me/N-Me (%), and ANS-Ptm (mm), explained 55.4% of the variation in profile attractiveness. This aligns with the perspective that "facial aesthetics require consideration of both bone and soft tissue". Among these, the H-angle alone explained 28.8% of the aesthetic variation, indicating its core role in determining profile attractiveness. When the H-angle approached 17.2°, profile attractiveness reached a relatively high level. The L1-APog measure explained 14.6% of the aesthetic variation, with an MAV of 0.5 mm, suggesting that the position of the lower incisors may affect aesthetic perception at the millimeter level, offering a new perspective for defining the scope of orthodontic compensatory treatment. The Wits appraisal explained 4.5% of the variation, with an MAV of 0.1 mm. This measure primarily assesses the anterior-posterior relationship between the maxilla and mandible, resulting in better facial coordination and aesthetics when it approaches 0.1 mm. The ANS-Me/N-Me measure explained 4.2% of the variation, with an MAV of 54%, indicating that public aesthetic perception is not only concerned with sagittal protrusion but also is influenced by the vertical proportions of the lower face. This requires clinicians to consider three-dimensional spatial coordination when formulating treatment plans [23, 24]. The ANS-Ptm measure explained 3.3% of the variation, with an MAV of 46.7 mm, demonstrating that maxillary length is important for maintaining facial aesthetics. Together, these five measures provide a comprehensive index system for predicting profile attractiveness. Their combined explanatory power is significantly greater than those of individual analyses, offering a powerful tool for more accurately predicting and guiding improvement in profile aesthetics.

Despite the meticulous design of the methodology of this study, there were several limitations. First, the evaluation of profile attractiveness relied primarily on subjective scoring by laypeople, which simulated public aesthetic perception but lacked a detailed analysis of aesthetic differences across diverse cultural backgrounds and age groups [25]. Future studies should refine the evaluator group to explore the roles of varying aesthetic concepts on facial attractiveness evaluations. Second, this study did not conduct racial subgroup analyses, and the model's generalizability requires validation through multicenter studies [26]. Future research could establish race-specific aesthetic prediction models using larger sample sizes.

In conclusion, among the nine cephalometric analyses, the Holdaway method shows the strongest explanatory power for variation in profile attractiveness. Individually, H-angle, ANB (°), A-Npog (mm), and NA-APo (°) each accounts for more than 26% of attractiveness variation and were highly correlated. The five-indicator predictive model, which integrates H-angle, L1-APog (mm), Wits appraisal (mm), ANS-Me/N-Me (%), and ANS-Ptm (mm), provides a new quantitative tool for setting aesthetic goals in orthodontic and orthognathic treatments.

Disclosure of conflict of interest

None.

Address correspondence to: Hongyu Ren, Department of Orthodontics, Xiangyang Stomatological Hospital, No. 6 Jianhua Road, Xiangyang 441003, Hubei, China. Tel: +86-18186280612; E-mail: renhongyu163@163.com; renhongyu@whu.edu.cn

References

[1] Kouskoura T, Ochsner T, Verna C, Pandis N and Kanavakis G. The effect of orthodontic treatment on facial attractiveness: a systematic review and meta-analysis. Eur J Orthod 2022; 44: 636-649.

[2] Oka A, Tanikawa C, Ohara H and Yamashiro T. Relationship between stigma experience and self-perception related to facial appearance in young Japanese patients with cleft lip and/or palate. Cleft Palate Craniofac J 2023; 60: 1546-1555.

[3] Liu C, Du S, Wang Z, Guo S, Cui M, Zhai Q, Zhang M and Fang B. Impact of orthodontic-induced facial morphology changes on aesthetic evaluation: a retrospective study. BMC Oral Health 2024; 24: 24.

[4] Malta LA, Baccetti T, Franchi L, Faltin K Jr and Mcnamara JA Jr. Long-term dentoskeletal effects and facial profile changes induced by bionator therapy. Angle Orthod 2010; 80: 10-17.

[5] Elbarnashawy SG, Keesler MC, Alanazi SM, Kossoff HE, Palomo L, Palomo JM and Hans MG. Cephalometric evaluation of deep overbite correction using anterior bite turbos. Angle Orthod 2023; 93: 507-512.

[6] Kim JH, Moon JH, Roseth J, Suh H, Oh H and Lee SJ. Craniofacial growth prediction models based on cephalometric landmarks in Korean

and American children. Angle Orthod 2025; 95: 219-226.
[7] Sycinska-Dziarnowska M, Lindauer SJ, Szyszka-Sommerfeld L, Spagnuolo G and Wozniak K. Laryngeal cartilage calcifications on lateral cephalometric radiographs. Sci Rep 2024; 14: 2388.
[8] Wang X, Mei M, Han G, Luan Q and Zhou Y. Effectiveness of modified periodontally accelerated osteogenic orthodontics in skeletal class ii malocclusion treated by a camouflage approach. Am J Transl Res 2022; 14: 979-989.
[9] Tweed CH. The frankfort-mandibular plane angle in orthodontic diagnosis, classification, treatment planning, and prognosis. Am J Orthod Oral Surg 1946; 32: 175-230.
[10] Burstone CJ. Lip posture and its significance in treatment planning. Am J Orthod 1967; 53: 262-284.
[11] Jacobson A. The "wits" appraisal of jaw disharmony. Am J Orthod 1975; 67: 125-138.
[12] Mcnamara JA Jr. A method of cephalometric evaluation. Am J Orthod 1984; 86: 449-469.
[13] Holdaway RA. A soft-tissue cephalometric analysis and its use in orthodontic treatment planning. Part I. Am J Orthod 1983; 84: 1-28.
[14] Marchiori GE, Sodre LO, da Cunha TCR, Torres FC, Rosario HD and Paranhos LR. Pleasantness of facial profile and its correlation with soft tissue cephalometric parameters: perception of orthodontists and lay people. Eur J Dent 2015; 9: 352-355.
[15] Ghorbanyjavadpour F and Rakhshan V. Factors associated with the beauty of soft-tissue profile. Am J Orthod Dentofacial Orthop 2019; 155: 832-843.
[16] Yu XN, Bai D, Feng X, Liu YH, Chen WJ, Li S, Han GL, Jiang RP and Xu TM. Correlation between cephalometric measures and end-of-treatment facial attractiveness. J Craniofac Surg 2016; 27: 405-409.
[17] Oh HS, Korn EL, Zhang X, Liu Y, Xu T, Boyd R and Baumrind S. Correlations between cephalometric and photographic measurements of facial attractiveness in Chinese and US patients after orthodontic treatment. Am J Orthod Dentofacial Orthop 2009; 136: 762, e1-14.
[18] Godinho J, Fernandes D, Pires P and Jardim L. Cephalometric determinants of facial attractiveness: a quadratic correlation study. Am J Orthod Dentofacial Orthop 2023; 163: 398-406.
[19] Kirschen RH, O'Higgins EA and Lee RT. The royal london space planning: an integration of space analysis and treatment planning: part I: assessing the space required to meet treatment objectives. Am J Orthod Dentofacial Orthop 2000; 118: 448-455.
[20] Hernandez-Sayago E, Espinar-Escalona E, Barrera-Mora JM, Ruiz-Navarro MB, Llamas-Carreras JM and Solano-Reina E. Lower incisor position in different malocclusions and facial patterns. Med Oral Patol Oral Cir Bucal 2013; 18: e343-e350.
[21] Ren H, Chen X and Zhang Y. Correlation between facial attractiveness and facial components assessed by laypersons and orthodontists. J Dent Sci 2021; 16: 431-436.
[22] Godinho J, Goncalves RP and Jardim L. Contribution of facial components to the attractiveness of the smiling face in male and female patients: a cross-sectional correlation study. Am J Orthod Dentofacial Orthop 2020; 157: 98-104.
[23] Naini FB, Moss JP and Gill DS. The enigma of facial beauty: esthetics, proportions, deformity, and controversy. Am J Orthod Dentofacial Orthop 2006; 130: 277-282.
[24] Farha P, Arqub SA and Ghoussoub MS. Correlation between cephalometric values and soft tissue profile in class I and class II adult patients based on vertical patterns. Turk J Orthod 2024; 37: 36-43.
[25] Musa M, Awad R, Mohammed A, Abdallah H, Elhoumed M, Al-Waraf L, Qu W, Alhashimi N, Chen X and Wang S. Effect of the ethnic, profession, gender, and social background on the perception of upper dental midline deviations in smile esthetics by Chinese and black raters. BMC Oral Health 2023; 23: 214.
[26] Uysal T, Baysal A, Yagci A, Sigler LM and Mcnamara JA Jr. Ethnic differences in the soft tissue profiles of Turkish and European-American young adults with normal occlusions and well-balanced faces. Eur J Orthod 2012; 34: 296-301.